ESRF	**Experiment title:** Nuclear inelastic scattering and nuclear reflectivity as probes for ion induced recrystallization in Fe60V40 thin films	E
Beamline: ID18	**Date of experiment**: from: 26.08.2022 to: 01.09.2022	**Date of report**: Preliminary report: 13.09.2022 *Received at ESRF:*
Shifts: 15	**Local contact(s)**: Aleksandr Chumakov	

Names and affiliations of applicants (* indicates experimentalists):

[1]Simon Rauls

[1]Benedikt Eggert

[1]Tom Helbig

[1]University of Duisburg-Essen, Faculty of Physics, AG Wende, Germany

Preliminary Report:

$Fe_{60}V_{40}$ thin films are promising candidates for the easy fabrication of magnetic nanostructures for spintronic and spin-wave applications. This is mainly because of 2 different things: on one hand, $Fe_{60}V_{40}$ thin films exhibit very low Gilbert damping and on the other hand they show a short-range-ordered, paramagnetic to polycrystalline, ferromagnetic phase transition, which can be locally triggered by ion irradiation. That means, it is possible to “write” ferromagnetic nanostructures into paramagnetic templates in a single irradiation step using focussed ion beams or broad beams with masks.
The aim of the experiment was to answer some pending questions about the ion induced phase transition by characterizing depth dependencies in the short-range-ordered thin films before and after irradiation with different ion fluences.
Other than planned in the original proposal, we measured both nuclear inelastic scattering in Θ-2Θ geometry and nuclear forward scattering in fluorescence with angular dependance for a wide array of samples. This includes a total of 10 samples in nuclear reflectivity and 5 samples total for nuclear inelastic scattering in different angular positions near the angle of total external reflection.. This was possible, due to the high quality of our samples (flat, low-roughness thin-films), enabling measurements nuclear forward scattering for adequate signal to noise ratio in 1-10 minutes and nuclear inelastic scattering with ~around 0.5 hours per scan, achieving 10^3 counts in the main phonon branch with mostly 1-3 scans. Some examples of the data are given below, namely nuclear forward scattering of an ion irradiated sample measured at different angles (a), as well as nuclear inelastic scattering curves of an amorphous sample, a sample irradiated with small ion fluence and a sample which was grown in a polycrystalline fashion (b).
For this preliminary report, we will only discuss the first, obvious conclusions.

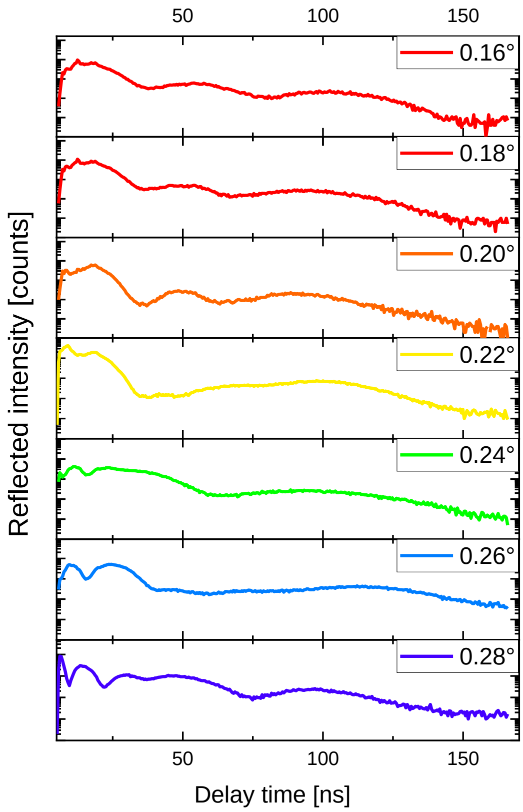

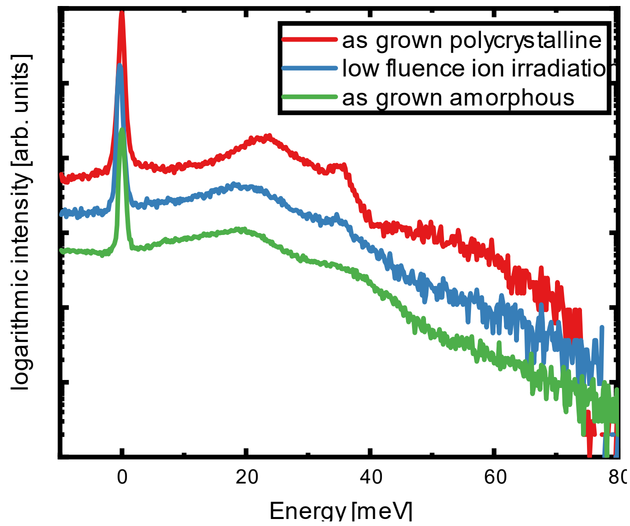

Figure 1: a) Nuclear forward scattering of an ion irradiated sample at different angles near the angle of total external reflection b) nuclear inelastic scattering for 3 samples: as-grown polycrystalline, ion irradiated and as grown amorphous. The blue and red curves are shifted towards the top, for better visibility.

In fig 1a), several nuclear reflectivity spectra can be seen for different incident angles Θ of the 14.4 keV incident beam, while the delayed signal was detected in an angle 2Θ in reference to the incident beam using the APD setup present at the beamline. For all samples measured, amorphous, as well as polycrystalline samples, we see non trivial interference patterns caused by various distributions of hyperfine interactions and different sublayers in the samples. This makes an accurate analysis of the reflectivity very difficult, which is why we apply for additional beamtime using the Synchrotron Mössbauer Source to measure the depth-dependence in the energy domain, to get an indication on how to model the nuclear forward scattering data. While for all samples, those difficult to interpret interferences show up, we can still see differences across all samples. As a first note, the first few nanometers show a thin oxide layer, which was previously seen in TEM images on similar samples and seems to be confirmed by the reflectivity measurements, as the smallest angular positions look similar across all samples. However, upon increase of the incident angle (and therefore penetration depth of the incoming synchrotron radiation) different patterns are observed for the various samples, indicating differences in the hyperfine interactions of the samples and in the depth-occurrence of different sublayers, which has to be further analysed.

In fig. 1b), three nuclear inelastic scattering spectra are shown for an amorphous as-grown sample, a polycrystalline, as-grown sample and a sample, irradiated with an ion fluence of $8*10^{14}$ Ne^{+} ions/cm^2, all measured in an incident angle of 0.288 degrees, where the whole thin-film is penetrated by the incident beam.

Clear distinctions in the visible features can alredy made out by eye. For the polycrystalline, as-grwon films, two distinct features in the spectrum can be made out, namely at 22.5 meV and at 35 meV. For amorphous and ion-irradiated samples, those features are increasingly broadened, indicating a not as well-defined crystallographic structure, which we will be able to compare with previously aquired EXAFS data. Furthermore, we can already observe shifts in those features, which, just like the depth-dependance in the nuclear inelastic scattering, we will have to analyze further.

All in all, it was a successful data, where, thanks to the kind help of our local contacts, we were able to aquire lots of good quality data. For the adequate modelling of the reflectivity spectra, we will need some additional depth-dependant information, which we hope to obtain in a future SMS beamtime at the same beamline. The inelastic scattering data however already looks promising for a deeper analysis of the ion-induced amorphous-polycrystalline phase-transition.